

<sup>1</sup> Shwetha G<sup>2</sup> Guruswamy K  
P

# An ANN-Fuzzy Based Single Phase PWM Rectifier for EV Application



**Abstract:** - With advancements in technology, numerous charging technologies for EV topology has been emerged. Various converters and Recently, several modeling strategies have been set forward to improve these chargers' performance. Among those, most frequent forms of rectifier is pulse width modulation (PWM). The single-phase converter, which transfers electric energy between the grid and battery pack, acts as less harmonic free. Input current can be decreased with PWM rectifiers. This paper proposes a pwm rectifier based on PI,ANN and Fuzzy controllers for control method and also refers Hysteresis and SPWM techniques for modulation purpose.The two stage conversion and battery management system are discussed.Simulation testing are conducted to examine the working of pulse width modulated rectifier in terms of rising time, settling time, power factor, harmonic distortion and efficiency. The experimental laboratory setup is executed to Validate the Results.

**Keywords:** Aartificial Nural Network, SPWM, PI controller, Fuzzy controller and Hysteresis Current control

## I. INTRODUCTION

The Electric vehicles (EV) driven by renewable energies to achieve clean and pollution free environment is emerging to ease the burden of energy scarcity [1]. In case of EV, Batteries play a significant role and are closely correlated with charging technologies in terms of charging time and battery life [2]. Onboard charging has grown to be a research hotspot in various electric car charging systems [3]. Because it may successfully protect batteries and increase their lifespan, single-phase charging is best popular charging methods used in residential settings [4-8]. There are a variety of single phase charging techniques, because of requirement of V2G applications and its controllability over charging current/ voltage. Single phase PWM rectifier related charging has garnered increasing attention. However, in this, during charging, both current and the voltage will produce a pulsing power [9-13].

The second harmonic pulsing current used in EV charging systems poses a risk to the batteries since it can increase electrochemical states of charge and overheat due to greater RMS current, and shorten battery life [14]. In most cases, a battery's current ripple should be less than 10% of its rated value [15-17]. Consequently, it is crucial to reduce ripple of both charging current/voltage of a battery [18] and 2<sup>nd</sup> harmonic ripple (voltage) at the rectifier output. Passive and active filtering are the two main techniques used to attenuate the 2<sup>nd</sup> harmonic ripples so far.

Two popular passive filtering techniques such as

- (i) installing large volume of DC capacitors
- (ii) incorporation of LC circuits.

However, the power density has been sacrificed because these AF call for more passive devices and switches in the charging system. Hence, to maintain the constant voltages at its output end, Controllers have been implemented. Several type control algorithms have been developed to enhance the dynamic response of rectifiers. In the control of PWM based rectifiers, most commonly PI controllers are most superior one because of its simplicity. However, mainly designing controller parameters, these controllers require a accurate mathematical model of the system. While in this manner they are most sensitive to parameter changes. So implementation of these analogue controllers is unsuitable for reliable performance. As a result, an artificial intelligence (AI) technique-based controller has played a significant role in industrial drive control. Several AI-based heuristic controls have since been developed.

Because of its automatic tuning capability, a fuzzy logic controller is becoming more popular among these. The parameters can also be tuned for a wide range, so crucially adjusted / tuned for a broad spectrum of changes in its operating condition. Hence, this work formulated a fuzzy controller in order to boost the execution of proposed rectifier.

A novel online grid voltage estimate method for sensorless PWM rectifier control. This method is predicated on basic adaptive neural networks (ANNs)[19-21]. The inherent noise immunity, online adaptability, high accuracy, simple implementation process, and minimal computational weight (single layer NN) of the suggested ANN estimator are its key advantages over alternative approaches. Furthermore, the control structure has no effect on the ANN estimator. As such, it is easily adaptable to various control schemes.

<sup>1</sup> Research Scholar, Electrical and Electronics Department, UVCE, K R circle, Bangalore University, Bangalore, India. m.g.shwetha99@gmail.com

<sup>2</sup> Associate Professor, Electrical and Electronics Department, UVCE, K R circle, Bangalore University, Bangalore, India. kpg\_eeuvce@bub.ernet.in

Copyright © JES 2024 on-line : journal.esrgroups.org

Table 1 shows how the combination of traditional and an intelligent controller can enhance the system's transient analysis and lessen the input current's overall harmonic distortion as compared to using only one controller. The comparison of several controllers is shown in Table 1. PFC [22], DPC [23], VOC [24] and DPC SVM [25] are the most often used power controllers in EV charging station.

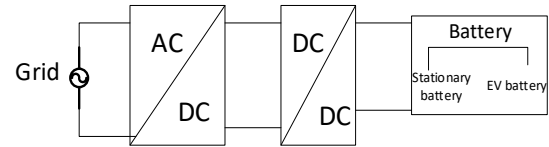
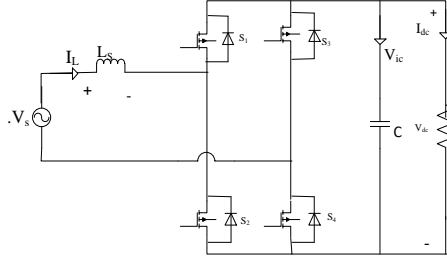
Table 1. Summary of controllers incorporated in EV charging

converter	controller	%THD
Bridge rectifier	PFC/ Current Controller	6.22
SEPIC Converter	GA based controller	1.68
Three phase rectifier	Direct Power Controller	2.01
Three phase controlled rectifier	DPC	4.6
Inverter	DPC	6.4
Three phase controlled rectifier	VOC	0.28
Three phase controlled rectifier	DPC SVM	4

This research proposes a single phase PWM rectifier with SPWM and hysteresis control topologies for EV charging system. The suggested solution incorporates fuzzy, ANN and PI controllers in EV charging stations. The proposed rectifier exhibits improved transient stability and THD of less than 5% when it incorporate MPC based method for switching signals. By dramatically lowering the input current and THD, the suggested design can outperforms AC-DC power conversion in high power applications.

## II. CONFIGURATION OF PROPOSED STRUCTURE

The proposed PWM rectifier structure is shown in Fig. 1(a). Four IGBT switches ( $S_1$ – $S_4$ ) make up the H-bridge rectifier, which is coupled to a rectifier power source through a series input inductor ( $L_s$ ). The DC voltage ( $V_{dc}$ ) is maintained constant by a dc-link capacitor ( $C$ ). The single-phase 50 Hz ac supply serves as the topology's input, and the input side of the line includes a boosting inductor. Every power switch, in this case an IGBT, blocks a voltage equivalent to voltage of the DC link. PWM signals for IGBT gate pulse are produced by commutating the switches at a high switching frequency. from Fig 1(b) which show the conversion of evergy from grid to storage of batteries gives source to load configuration.



(b). Layout of Grid to Battery charging conversion

Figure 1 (a). Proposed PWM rectifier

The voltage across the input inductor ( $L$ ) can be calculated by applying KVL.

$$V_s = L_s \frac{di_s}{dt} + V_{dc} \quad (1)$$

$$L_s \frac{di_s}{dt} = v_s - v_{ab} - i_s R_s \quad (2)$$

AC side voltage can be given as

$$v_s(t) = V_s \cos(\omega t) \quad V_s = V_c \cos \delta \quad (3)$$

Line current can be represented as

$$i_s(t) = I_s \cos(\omega t - \varphi) + \sum_{k=3,5,7,\dots}^{\infty} I_{SK} \cos(k\omega t - \varphi_k) \quad (4)$$

$$I_s \sin \theta = \frac{V_s - V_c \cos \delta}{x_s} \quad (5)$$

Where,

$u_s$  – AC voltage;

$i_s$  – AC current  
 $u_{AB}$  - Rectifier voltage  
 $\omega$  - angular frequency  
 $\psi$  - Power factor angle.

### III. MODULATION TECHNIQUE AND CONTROLLER DESIGN

#### A. SPWM technique (Sinusoidal Pulse Width Modulation)

Sinusoidal PWM is a commonly used PWM technique. The triangular carrier wave and the reference sinusoidal AC voltage are compared in this PWM technique to determine the switching states for each pole. The fig 2 presents the SPWM and different mode of intervals. The foundation of sinusoidal modulation is a triangle carrier signal. Comparing this triangle wave to three sinusoidal reference voltages is a concept. In contrast, the power transistor's switching instants are defined by the logical signals operation with concentrated voltage harmonics around the switching frequency and multiples of the switching frequency due to a continuous carrier signal.

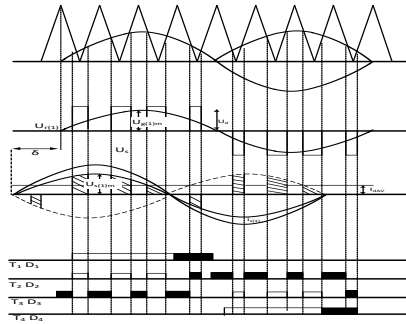


Figure 2. sinusoidal pulse width modulation waveform

#### B. Hysteresis Current Controller (HCC)

The voltage source rectifier operated by conventional HCC compares the current error ( $e(t)$ ) with the fixed hysteresis bands. Fig 3 gives pulse generation from HCC. the hysteresis function output is used for switching hardware operation. the setting current and the real currents are two different parts assumed as input for hysteresis function. By comparing the obtained result which is the difference with hysteresis threshold becomes the signal for driving power switches.

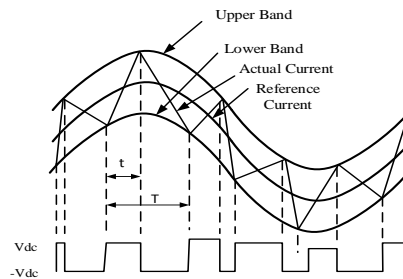


Figure 3. Hysteresis control for pulse generation

#### C. Artificial Neural Network (ANN)

In this work, a new artificial neural network (ANN) technique is developed for estimating the appropriate duty cycle for a perfect match between grid voltage and grid current, resulting in unity power factor. Hence to develop and execute a neural network by working with one input layer, one hidden layer, and one output layer; however, multiple hidden layers may be included. The ANN's basic building block, the neuron, is depicted in Fig 4 along with its several processing stages, which are represented by the input variable receiving stage, the variable weighting stage, the adder stage, and the Z value also indicated. Any one of the three activation functions can change this value.

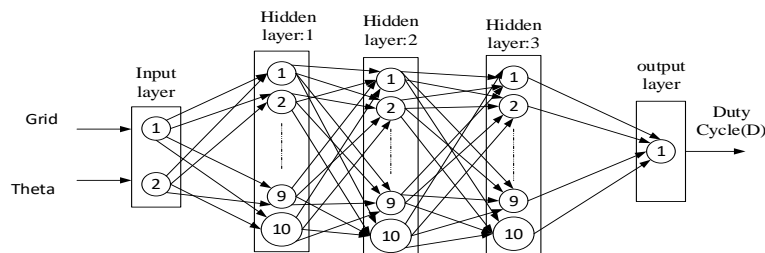


Figure 4. Design of Artificial Neural network Controller

#### D. PI Controller

The most popular type of controller for industrial applications is the PI controller, which performs well under a variety of operating situations. Fig.5 follow-up the PI used in AC-DC converter. For a sinusoidal reference, PI controllers are intrinsically unable to provide zero steady state control error. Only when the reference value remains constant in a steady state the integral action eliminate the inaccuracy. The current measurements are converted to DC quantities using the Clarke and Park transformations, after which a straightforward PI controller can produce satisfactory results. For the linked system, a PI current controller does not provide adequate tracing performance. It is necessary to cancel this cross-coupling in order to track current with high performance and precision

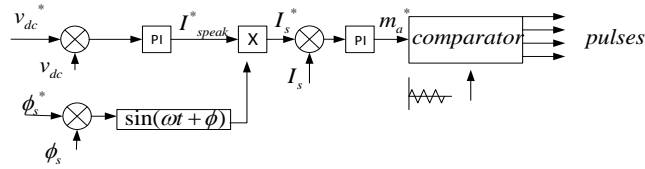


Figure 5. Design of Proportional Integral Controller

$$G_{PI}(s) = K_p + \frac{K_I}{s} \quad (6)$$

#### E. Fuzzy Logic Controller (FLC)

Intelligent systems known as FLCs are distinguished by their language representations derived from specific information. Fuzzification is the process of transforming crisp values into fuzzy values. Membership functions (MFs) are used to describe this conversion of fuzzy values. A frequently utilized membership function is the triangle membership function. Its simplicity is the main justification for its selection. The purpose of the rule base is to formulate its output. Linguistic variables are used by the rule-base to create its antecedents and consequents. An error and its change in error will be the fuzzy controller's inputs.

The two inputs of the FLC are the error  $e(r)$  and change of error  $ce(r)$  are described in equations 7 and 8 respectively as, and the representation is shown in Fig.6.

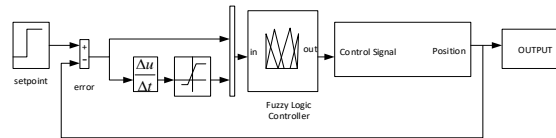


Figure 6. Fuzzy logic controller

$$e(r) = x(r) - y(r) \quad (7)$$

$$ce(r) = e(r) - e(r-1) \quad (8)$$

Where

$x$  -reference input;

$y$  -system output;

$r$  - present state

$(r-1)$  - previous state.

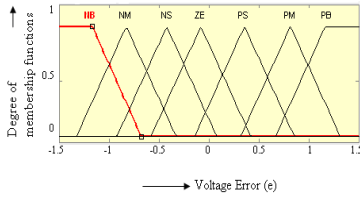
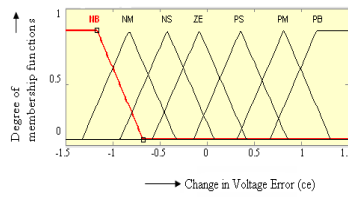
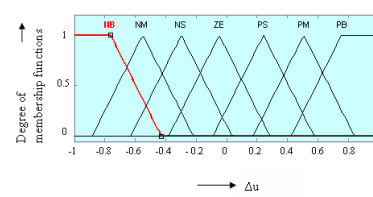
The rule base is evaluated as inputs that are received by the FLC. The FLC's output is the incremental change in the control signal  $cu(r)$ . The process generates these outputs. Another name for defuzzification is the "rounding off" technique. It condense the values of the membership function into a single quantity. Because of its precision, the Centroid technique is used for defuzzification in this work.

As a result, the FLC used in this framework has:

- Seven fuzzy sets with triangle membership functions for each input ( $e$ ,  $\Delta e$ ) and output ( $\Delta u$ ).
- CoD for fuzzification.

- 'min' operator of Mamdani's implications.
- Utilized "centroid" approach for defuzzification

By examining the error ( $e$ ) and change in error ( $e^*$ ), the input to FLC is determined. The previous error condition is the adjustment in error. Here Triangle membership is selected and the Mamdani technique is applied. A membership work is characterized by five language elements. The number of fuzzy language factors is not well-established and depends on the necessary input determination. Positive Big (PB), Positive Small (PS), Zero (ZE), Negative Small (NS), and Negative Big (NB) are the several types of big. A fuzzy subset is the fuzzy controller's output. To convert the linguistic fuzzy set back into actual value, use the defuzzifier. The triangular MF of input and output variables are shown in Figures 7a, 7b and 7c respectively.

Figure 7a. MF for  $e$ Figure 7b. MF for  $\Delta e$ Figure 7c. MF for  $\Delta u$ 

#### IV. RESULTS AND DISCUSSION

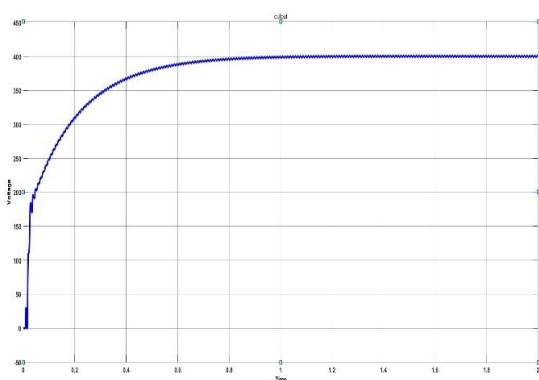
This section includes a simulation test to assess the dynamic performance of proposed PWM rectifier topology. An analysis of the control method examined in this study was verified using a numerical simulation conducted in the MATLAB/SIMULINK environment. The primary electrical control data and power circuit characteristics utilized for experiment listed in Table 2 the PWM rectifier's parameters that were employed in the simulation investigation.

**Table 2. Parameters for Converter**

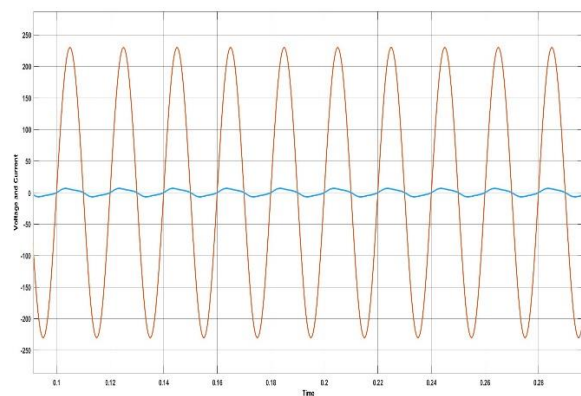
Parameters	Values
Input Voltage	230AC, 50 Hz
Output Voltage	400 V
Inductor (Ls)	2mH
Capacitor	2000

##### A Results Obtained from Hysteresis control method:

As depicted in Fig.8 8a and 8b, the test is carried out in steady state operation. PWM rectifier's reference DC voltage is 400 V as given in 8a. and inputside measurement in fig 8b. the PI controller overshoots (almost) the reference DC voltage after 2.5sec. To ensure the stability of the closed-loop system, the pole compensation method is used to determine the parameters of the PI-dc voltage controller.



(a) Dc Output Voltage



(b) Input characteristics

**Figure 8. Output obtained with PI controller**

Additionally, Fuzzy system results in the input currents have waveforms which are sinusoidal and in phase with the voltage. The suggested controller, as can be shown in Fig. 9a, reaches reference DC voltage after 0.06 sec without overshoot is presented in fig.9b. The suggested control strategy also has a power factor of 1. Supply current is in phase with grid voltage, resulting unity power factor achieved.

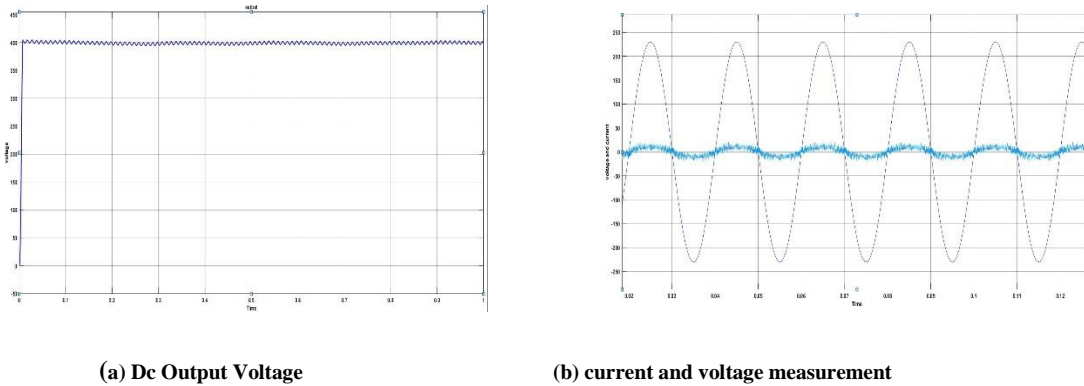


**Figure 9 (a) Output obtained with Fuzzy controller and (b) Input side waveform.**

From the fig 10a and 10b line currents are in phase with the voltages of the power source and extremely similar to sine waves. Successful UPF operation and good dc-bus voltage regulation achieved and the suggested neural network based controller gives more advantages, that it utilizes a neural network to select The converter's switching state is more effective than the traditional one.

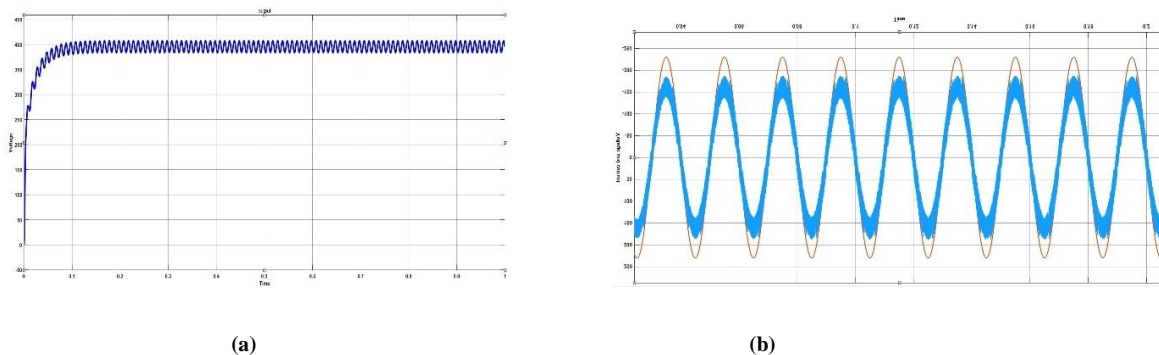


**Figure 10 (a) ANN controller based output and (b) Input side waveform from neural network adopted.**

It is clear from the performance that ANN-FLC performs better than PI in terms of settling time and maximum peak over-shoot for steady state operation which is experimented. a reliable neural network for the single phase PWM rectifier utilizing the ANN toolbox, using MATLAB simulation gives that The results demonstrate that, both in steady and transient states, the new. The ANN-Fuzzy results provide almost sinusoidal line current waveforms and a respectable increase in reducing active power and current ripples in steady state adaptability.

#### B Results from SPWM method:

While the results with SPWM technique are shown below. from the fig 11a which gives the output side voltage that reaches the steady state condition within 0.05 sec. where as fig 11b Represents the grid side waveform confirm the unity power factor and the less harmonic pollution of source side. hence the power quality issues are somehow sorted in Rectifier circuit. and the table 3 shows tabulation matrices in terms of rise time, settling time, PF and efficiency of different controllers and Modulation Control schemes.

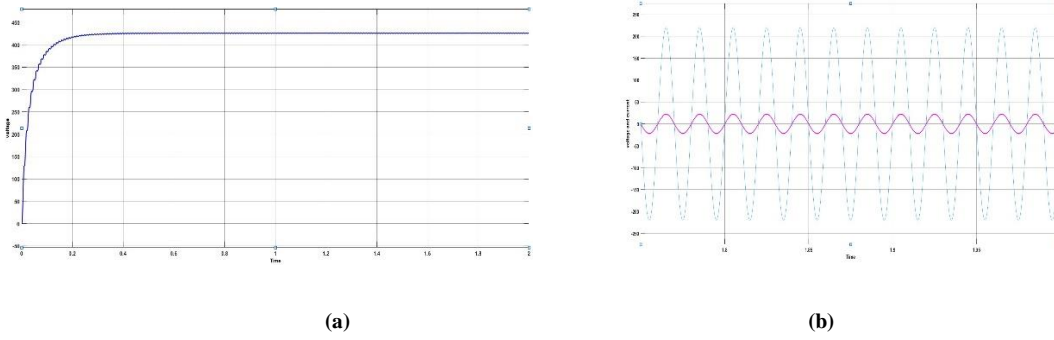


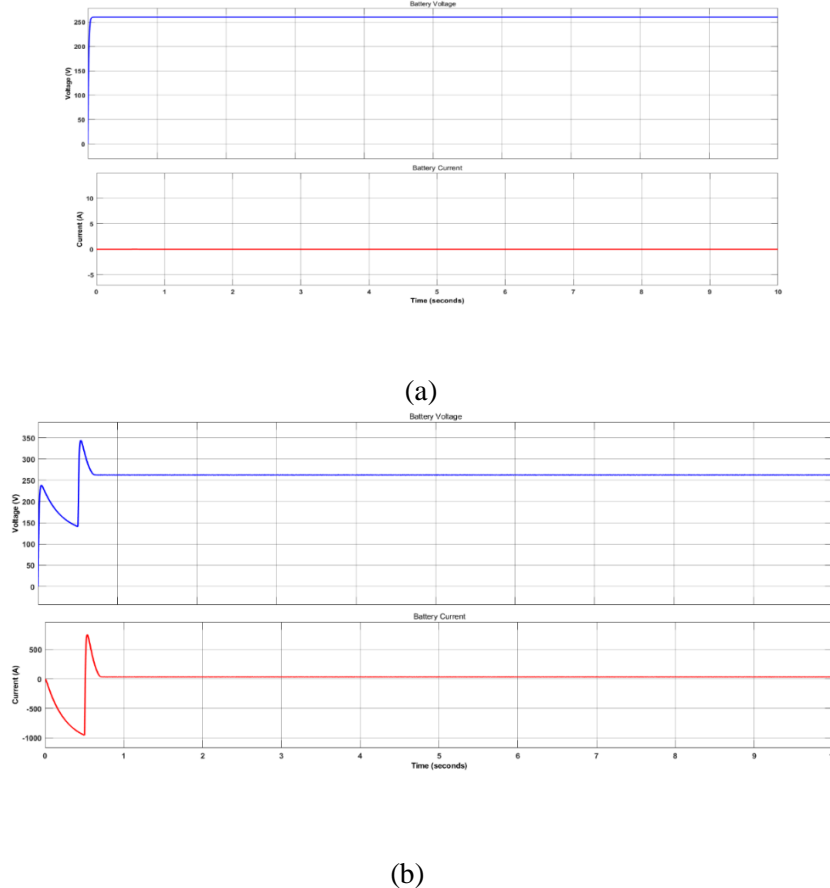
**Figure 11 (a) PI controller based output and (b) Input side measurement.**

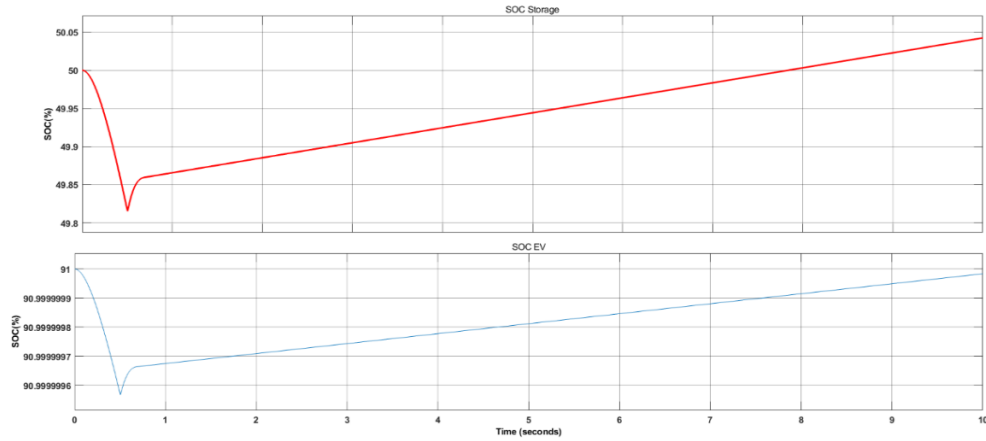
**Table 3.** Different rising time, settling time, power factor, harmonic distortion and efficiency of two methods.

Modulation technique	vin	vout	controller	Rise time	Settling time	PF	efficiency
Hysteresis (open loop)	230	400	-	0.04	0.2	0.922	89
Hysteresis	230	398	PI	0.045	0.05	0.921	92
Hysteresis	230	400	Fuzzy	0.005	0.009	0.95	94
SPWM(open loop)	230	415	-	0.05	0.31	1.04	80
SPWM	230	395	PI	0.012	0.02	0.89	88
SPWM	230	400	Fuzzy	0.009	0.01	0.911	90

### C Battery Management System

The working of battery i.e EV and stationary are graphically shown in Fig.12 a, b and c. while SOC and power measurement are also recorded. The conversion of two level energy i.e AC-DC,DC-DC and finally the storage and battery management system in Electric Vehicle and stationary battery are explained from the results fig 12a and 12b which gives the voltage and current waveforms of both batteries and fig 12c depicts State of charge.





(c)

Figure 12. (a) Voltage and current measurements of EV battery, (b) V and I of stationary battery and (c) SOC.

#### D Hardware Implimentation

The Hardware blueprint is elucidated in Fig 13. And components required is also predicted. the pulses generated from SPWM modulation technique is predicted in fig 14 and pulses from both cycles are shown. where as from fig 15 input side voltage and current waveform that confirms that both are in phase are graphically presented. the output side dc voltage and current outcomes from the converter is depicted in fig 16. hence the proposed converter matches the Experimentation of laboratory setup results that matches with simulation pattern.

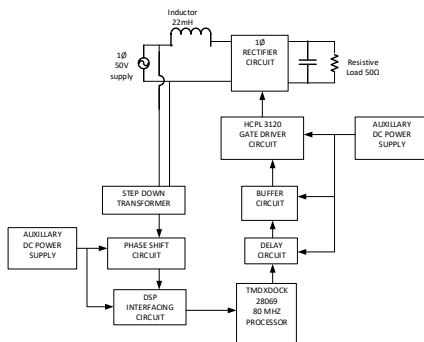


Figure 13. Hardware implementation

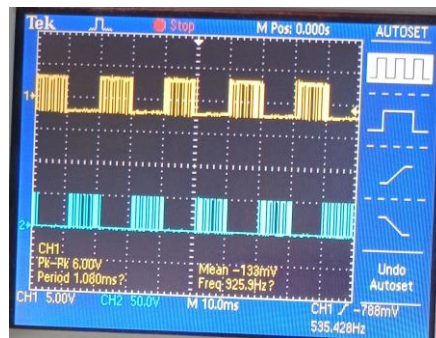


Figure 14. Pulses Generated from SPWM modulation technique

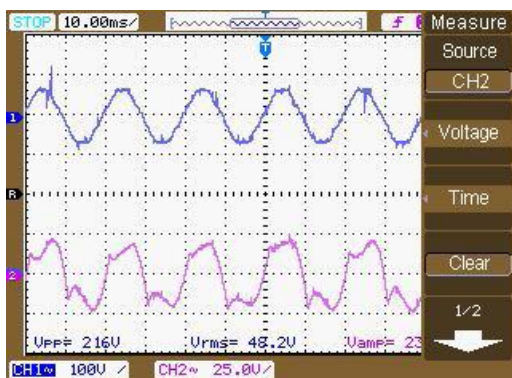


Figure 15. Input side voltage and current waveform.

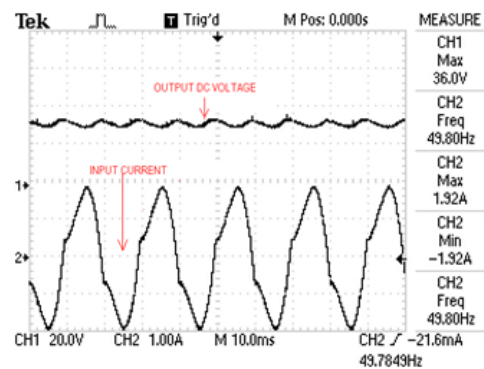


Figure 16. output side voltage and current waveform.



## V. CONCLUSION

In this work, an ANN, FLC and PI controller based PWM rectifier are suggested due to most suitable applications for EV charging station. And battery management system with two stage energy flow of EV and stationary batteries also discussed in depth. Simulation testing are executed at the same time for all controllers in the MATLAB environment. Simulation results show that the Referred control strategy provides more superior ANN-Fuzzy scheme performs better in terms of rise time, settling time and overshoot. Hence, it has to be proven that it is more suitable for EV charging station. while compared to conventional PI the suggested system gives more predominant Results.

## REFERENCES

- [1] Y. Su, X. Ge, D. Xie and K. Wang, "An Active Disturbance Rejection Control-Based Voltage Control Strategy of Single-Phase Cascaded H-Bridge Rectifiers," in *IEEE Transactions on Industry Applications*, vol. 56, no. 5, pp. 5182-5193, Sept.-Oct. 2020.
- [2] D. Kim, M. Kim and B. Lee, "An Integrated Battery Charger With High Power Density and Efficiency for Electric Vehicles," *IEEE Trans. Power Electron.*, vol. 32, no. 6, pp. 4553-4565, June 2017.
- [3] C. Shi, Y. Tang and A. Khaligh, "A three-phase integrated on board charger for plug-in electric vehicles," *IEEE Trans. Power Electron.*, vol. 33, no. 6, pp. 4716-4725, June 2018.
- [4] D. Kim, M. Kim and B. Lee, "An integrated battery charger with high power density and efficiency for electric vehicles," *IEEE Trans. Power Electron.*, vol. 32, no. 6, pp. 4553-4565, June 2017.
- [5] M. Yilmaz and P. T. Krein, "Review of battery charger topologies, charging power levels, and infrastructure for plug-in electric and hybrid vehicles," *IEEE Trans. Power Electron.*, vol. 28, no. 5, pp. 2151-2169, May 2013.
- [6] D. Thimmesch, "An SCR inverter with an integral battery charger for electric vehicles," *IEEE Trans. Ind. Appl.*, vol. IA-21, no. 4, pp. 1023-1029, Jul. 1985.
- [7] W. Lhomme et al., "Integrated traction/charge/air compression supply using three-phase split-windings motor for electric vehicles," *IEEE Trans. Power Electron.*, vol. 33, no. 11, pp. 10003-10012, Nov. 2018.
- [8] i.Subotic, N. Bodo, E. Levi, M. Jones and V. Levi, "Isolated chargers for EVs incorporating six-phase machines," *IEEE Trans. Ind. Electron.*, vol. 63, no. 1, pp. 653-664, Jan. 2016.
- [9] S. S. Zhang, —The effect of the charging protocol on the cycle life of a Li-ion battery, *J. Power Sources*, vol. 161, no. 2, pp. 1385-1391, Oct. 2006.
- [10] P. T. Krein and R. S. Balog, —Cost-effective hundred-year life for singlephase inverters and rectifiers in solar and LED lighting applications based on minimum capacitance requirements and a ripple power port, *Appl. Power Electron. Conf., APEC*, pp. 620-625, 2009.
- [11] M. Ecker et al., —Development of a lifetime prediction model for lithiumion batteries based on extended accelerated aging test data, *J. Power Sources*, vol. 215, pp. 248-257, 2012.
- [12] S. Bala, T. Tegnér, P. Rosenfeld and F. Delince, "The effect of low frequency current ripple on the performance of a Lithium Iron Phosphate (LFP) battery energy storage system," in *Proc. IEEE ECCE*, Sep. 15-20, 2012, pp. 3485-3492.
- [13] H. Wen, W. Xiao, X. Wen, and A. Peter, —Analysis and evaluation of DClink capacitors for high power density electric vehicle drive systems, *IEEE Trans. Veh. Technol.*, vol. 61, no. 7, pp. 2950-2964, Sep. 2012.
- [14] W. Chen and S. Hui, —Elimination of an electrolytic capacitor in AC/DC light-emitting diode (LED) driver with high input power factor and constant output current, *IEEE Trans. Power Electron.*, vol. 27, no. 3, pp. 1598-1607, Mar. 2012.
- [15] Z. Qin, Y. Tang, P. C. Loh, and F. Blaabjerg, —Benchmark of AC and DC active power decoupling circuits for second-order harmonic mitigation in kilowatt-scale single-phase inverters, *IEEE J. Emerg. Sel. Topics Power Electron.*, vol. 4, no. 1, pp. 15-25, Mar. 2016.
- [16] Y. Sun, Y. Liu, M. Su, W. Xiong, and J. Yang, —Review of active power decoupling topologies in single-phase systems, *IEEE Trans. Power Electron.*, vol. 31, no. 7, pp. 4778-4794, Jul. 2016.
- [17] S. Narula, B. Singh, and G. Bhuvaneswari, ``Power factor corrected welding power supply using modi\_ed zeta converter," *IEEE J. Emerg. Sel. Topics Power Electron.*, vol. 4, no. 2, pp. 617\_625, Jun. 2016.
- [18] S. Vazquez, J. A. Sanchez, J. M. Carrasco, J. I. Leon, and E. Galvan, ``A model-based direct power control for three-phase power converters," *IEEE Trans. Ind. Electron.*, vol. 55, no. 4, pp. 1647\_1657, Apr. 2008.
- [19] A.S. Al-Ogaili, I. B. Aris, R. Verayiah, A. Ramasamy, M. Marsadek, N. A. Rahmat, Y. Hoon, A. Aljanad, and A. N. Al-Masri, ``A three-level universal electric vehicle charger based on voltage-oriented control and pulse-width modulation," *Energies*, vol. 12, no. 12, p. 2375, Jun. 2019.
- [20] M. Malinowski, M. Jasinski, and M. P. Kazmierkowski, ``Simple direct power control of three-phase PWMrectifier using space-vector modulation (DPC-SVM)," *IEEE Trans. Ind. Electron.*, vol. 51, no. 2, pp. 447\_454, Apr. 2004.
- [21] W. Qi, S. Li, S.-C. Tan, and S. Y. Hui, ``Design considerations for voltage sensorless control of a PFC single-phase rectifier without electrolytic capacitors," *IEEE Trans. Ind. Electron.*, vol. 67, no. 3, pp. 1878\_1889, Mar. 2020.

- [22] S. Durgadevi and M. G. Umamaheswari, "Analysis and design of single phase power factor correction with DC\_DC SEPIC converter for fast dynamic response using genetic algorithm optimised PI controller," *IET Circuits, Devices Syst.*, vol. 12, no. 2, pp. 164\_174, Mar. 2018.
- [23] Y. Gui, M. Li, J. Lu, S. Golestan, J. M. Guerrero, and J. C. Vasquez, "A voltage modulated DPC approach for three-phase PWM rectifier," *IEEE Trans. Ind. Electron.*, vol. 65, no. 10, pp. 7612\_7619, Oct. 2018.
- [24] H. Nian, Y. Shen, H. Yang, and Y. Quan, "Flexible grid connection technique of voltage-source inverter under unbalanced grid conditions based on direct power control," *IEEE Trans. Ind. Appl.*, vol. 51, no. 5, pp. 4041\_4050, Sep. 2015.
- [25] M. Moallem, B. Mirzaeian, O. A. Mohammed, and C. Lucas, "Multi objective genetic-fuzzy optimal design of PI controller in the indirect field oriented control of an induction motor," *IEEE Trans. Magn.*, vol. 37, no. 5, pp. 3608\_3612, 2001